Antifungal activity and mechanism of novel peptide *Glycine max* antimicrobial peptide (GmAMP) against fluconazole-resistant *Candida tropicalis*

Ruxia Cai[1,*], Na Zhao[1,2,*], Chaoqin Sun[1], Mingjiao Huang[1,3], Zhenlong Jiao[1,3], Jian Peng[1,2], Jin Zhang[4] and Guo Guo[1,2]

[1] School of Basic Medical Sciences, Guizhou Key Laboratory of Microbial and Infectious Disease Prevention & Control, Guizhou Medical University, Guiyang, Guizhou, China
[2] Key Laboratory of Environmental Pollution Monitoring and Disease Control (Guizhou Medical University), Ministry of Education, Guiyang, Guizhou, China
[3] Translational Medicine Research Center, Guizhou Medical University, Guiyang, Guizhou, China
[4] School of Public Health, Guizhou Medical University, Guiyang, Guizhou, China
[*] These authors contributed equally to this work.

ABSTRACT

Background: There is a pressing need to create innovative alternative treatment approaches considering the overuse of antifungal drugs causes the number of clinically isolated fluconazole-resistant *Candida* species to increase. *Glycine max* antimicrobial peptide (GmAMP) is a novel peptide screened by us using artificial intelligence modeling techniques, and pre-tests showed its strong antimicrobial activity against clinically fluconazole-resistant *Candida tropicalis*.

Methods: The study aimed to comprehensively investigate the antimicrobial activity and mechanisms of GmAMP against fluconazole-resistant *C. tropicalis*. The antifungal activity of GmAMP against fluconazole-resistant *C. tropicalis* was assessed by using broth microdilution method, growth and fungicidal kinetics, hypha transformation, and antibiofilm assay. To further uncover the potential mechanisms of action of GmAMP, we performed scanning electron microscopy, flow cytometry, cell membrane potential probe 3, 3′-Dipropylthiadicarbocyanine Iodide ($DiSC_3(5)$), and reactive oxygen species (ROS) probe 2′, 7′-Dichlorodihydrofluorescein diacetate (DCFH-DA) detection to assess the cellular morphology and structure, membrane permeability, membrane depolarization, and ROS accumulation, respectively. At the same time, we used cytotoxicity and degree of erythrocyte hemolysis assays to assess GmAMP's toxicity *in vitro*. Cytotoxicity and treatment efficacy were evaluated *in vivo* by utilizing the *Galleria mellonella* larvae infection model.

Results: GmAMP exhibited significant antifungal activity against fluconazole-resistant *C. tropicalis* with a minimum inhibitory concentration (MIC) of 25 μM and demonstrated fungicidal effects at 100 μM within 2 h. GmAMP prevented the transition from yeast to hypha morphology, inhibited the biofilm formation rate of 88.32%, and eradicated the mature biofilm rate of 58.28%. Additionally, GmAMP treatment at 100 μM caused cell structure damage in fluconazole-resistant *C. tropicalis*, whereas GmAMP treatment at concentrations ranging from 25 to 100 μM caused membrane permeability, depolarization of cell membrane potential, and intracellular ROS accumulation. Moreover, GmAMP

Submitted 18 November 2024
Accepted 4 April 2025
Published 20 May 2025

Corresponding author
Guo Guo, guoguojsc@163.com

Academic editor
Nancy Keller

Additional Information and Declarations can be found on page 19

DOI **10.7717/peerj.19372**

How to cite this article Cai R, Zhao N, Sun C, Huang M, Jiao Z, Peng J, Zhang J, Guo G. 2025. Antifungal activity and mechanism of novel peptide *Glycine max* antimicrobial peptide (GmAMP) against fluconazole-resistant *Candida tropicalis*. **PeerJ 13:e19372**
DOI 10.7717/peerj.19372

enhanced the survival rate of 75% for *G. mellonella* with fluconazole-resistant *C. tropicalis* infection as well as reduced fungal burden *in vivo* by approximately 1.0×10^2 colony forming units per larva (CFU per larva).
Conclusion: GmAMP can disrupt the cell membrane of fluconazole-resistant *C. tropicalis* and also shows favorable safety and therapeutic efficacy *in vivo*. Accordingly, GmAMP has the potential to be an agent against drug-resistant fungi.

Subjects Microbiology, Mycology, Drugs and Devices, Epidemiology, Pathology
Keywords Antimicrobial peptide, GmAMP, Drug-resistance, Antifungal activity, *Candida tropicalis*

INTRODUCTION

Opportunistic fungal pathogens can cause cutaneous infections and invasive infections, posing a significantly higher risk of morbidity and mortality in immunocompromised patients (*Pathakumari, Liang & Liu, 2020*). Among these pathogens, invasive candidiasis emerges as a prominent concern, characterized by mortality rates of approximately 25% (*Pfaller & Diekema, 2007*; *Sasani et al., 2021*). Despite being a component of human microbiomes, *Candida tropicalis* is considered to be the second to fourth most virulent genus of *Candida* species and may result in invasive infections (*Zuza-Alves, Silva-Rocha & Chaves, 2017*). Azole antifungal agents, including fluconazole, itraconazole, voriconazole, posaconazole, and others, constitute the primary therapeutic resources against *C. tropicalis* infection. However, the indiscriminate and excessive use of azoles has engendered the emergence of azole-resistant strains of *C. tropicalis* from clinical isolates. In addition, compared to other *Candida* species, *C. tropicalis* showed a greater rate of fluconazole resistance, according to epidemiologic research (*Tseng et al., 2022*). Consequently, the significant prevalence of azole resistance in clinical isolates of *C. tropicalis* has drawn more attention to invasive infection (*Fan et al., 2023*). *C. tropicalis* was included as a high-priority pathogen in the World Health Organization's (WHO) first list of fungal priority pathogens in 2022, which was intended to create a strategic framework for research, development, and public health interventions (*Fisher & Denning, 2023*; *World Health Organization (WHO) ARDA, Control of Neglected Tropical Diseases (NTD) & Global Coordination and Partnership (GCP), 2022*).

It is widely recognized that azoles, fluconazole in particular, are crucial are essential preventive and therapeutic medicines for the management of *Candida* infections. Despite the widespread and regular use of fluconazole, resistance is increasing, which has caused the emergence of cross-resistance to other antifungal medications (*Forastiero et al., 2013*). Studies have shown that resistance rates of *C. tropicalis* to azoles such as fluconazole, itraconazole, voriconazole, and posaconazole have recorded resistance rates as high as 40% to 80% (*World Health Organization (WHO) ARDA, Control of Neglected Tropical Diseases (NTD) & Global Coordination and Partnership (GCP), 2022*). Furthermore, more than 21% of *C. tropicalis* isolates in China are resistant to fluconazole and even 21.7% of *C. tropicalis* isolates were resistant to 2–4 azoles in Iran (*Badiee et al., 2022*; *Liu et al., 2022*). A number of mechanisms, such as changes in drug targets, elevation of drug target expression, and

increased expression of efflux pumps, may be responsible for the resistance phenomena (*Lee et al., 2021*). As a result, antifungal drug therapies may be inefficient in treating drug-resistant candidiasis, which poses significant challenges in clinical management (*McCarthy & Walsh, 2017*; *Zhang et al., 2017*). In order to address the current issue of fungal drug resistance, it is imperative to utilize both novel and promising antifungal medicines as well as alternative treatment techniques.

Antimicrobial peptides (AMPs) represent critical components of the immune defense system in organisms, with broad-spectrum antimicrobial activity, low drug resistance, and diverse bactericidal mechanisms (*Li et al., 2020*). Antimicrobial peptides can destroy multiple targets of pathogens through membrane and non-membrane interactions, which differs from the single target bactericidal principle of conventional antibiotics. The membrane destructive effect is primarily exerted through three mechanisms: barrel-stave, toroidal or carpet, these unique mechanism makes it not easily susceptible to the development of resistance (*Gan et al., 2021*). We have previously reported that we employed multitasking adaptive modeling and model adaptation to establish a prediction model and screening protocol for antifungal peptides based on antimicrobial peptide databases such as APD, DRAMP, CAMP, antifp, *etc.* (*Zhang et al., 2022*). Then we predicted more than three million unknown functional sequences in the UniProt database from the established model and screened out several hundreds of peptides that might be antifungally active then synthesized them by solid-phase organic synthesis method, and the antimicrobial activity was verified by wet lab experiments. The novel antimicrobial peptide SPGKKKKKKKKKKTKKKKKK showed strong antimicrobial activity against fluconazole-resistant *C. tropicalis* in the pre-test, with a minimum inhibitory concentration (MIC) of 25 μM (MIC of fluconazole against this isolate >3,343 μM).

According to the sequence homology nomenclature in the antimicrobial peptide APD3 database (http://aps.unmc.edu/AP/), the *Glycine max* antimicrobial novel peptide was named GmAMP. In this report, to more fully assess GmAMP, we first determined the MIC of GmAMP against four strains of clinically fluconazole-resistant *C. tropicalis* and the standard strain of *C. tropicalis* ATCC 20962, for which GmAMP showed excellent antimicrobial activity. Besides, to assess the antifungal activity and mechanism of GmAMP, we performed experimental validation on fluconazole-resistant *C. tropicalis*. As a result, the antifungal mechanism of GmAMP against fluconazole-resistant *C. tropicalis* was investigated in terms of physicochemistry and morphology, and its *in vivo* efficacy was evaluated by the *G. mellonella* larvae infection model. Thus, the findings of this study provide a certain experimental foundation for the exploration and utilization of novel peptide antimicrobial drugs.

MATERIALS AND METHODS

Materials

The peptide GmAMP (SPGKKKKKKKKKKTKKKKKK) was synthesized by solid phase chemical synthesis method by Gil Biochemical Co., Ltd (Shanghai, China), purified by reversed-phase high-performance liquid chromatography (RP-HPLC) (Fig. S1A), and the purity was >95%. They were dissolved in deionized water at a stock concentration of

5 mg/mL before use. The molecular weight of GmAMP was determined using electrospray ionization (ESI) mass spectrometer (ESI MS) (Fig. S1B). We used the online website Heliquest software (https://heliquest.ipmc.cnrs.fr/index.html) to predict the helix diagram and hydrophilicity, and AlphFold2 to predict the 3D structure of peptides. The molecular weight of the peptide was predicted by Expasy ProtParam (https://web.expasy.org/protparam/).

Strains and cell culture conditions

The fluconazole-resistant *C. tropicalis* 4171, 4252, 6984, and 8402 were collected from infected patient's blood in the affiliated hospital of Guizhou Medical University. *C. tropicalis* ATCC 20962 was purchased from the Shanghai Conservation Biotechnology Center. All strains were grown in yeast extract peptone dextrose medium (YPD, Solarbio, Beijing, China) at 35 °C with shaking at 200 rpm until the cultures reached the logarithmic phase. RPMI-1640 (Invitrogen, Carlsbad, CA, USA) supplemented with 15% fetal bovine serum (FBS) (Sigma-Aldrich) was used as the culture medium for hypha growth of *C. tropicalis*. The mouse monocyte-macrophage cell line RAW 264.7 was donated by Jiahong Wu from the Key and Characteristic Laboratory of Modern Pathogen Biology, Guizhou Medical University, and cells were cultured in DMEM medium (Gibco, Waltham, MA, USA) containing 10% fetal bovine serum (FBS, Gibco), 100 U/mL penicillin (Gibco, Waltham, MA, USA), and 100 μg/mL streptomycin (Gibco, Waltham, MA, USA) and maintained at 37 °C in a humidified 5% CO_2 incubator.

Antifungal activity

The minimum inhibitory concentration (MIC) of GmAMP for four fluconazole-resistant *C. tropicalis* from clinical isolates, and a standard strain of *C. tropicalis* ATCC 20962 was determined by using broth microdilution method according to the Standards of Clinical and Laboratory Standards Institute (CLSI) (*Clinical and Laboratory Standards Institute (CLSI), 2023*). In brief, these yeasts of fungal strains were cultured in YPD broth medium at 35 °C to the logarithmic growth stage, and the cultures were washed by phosphate-buffered saline (PBS, 10 mM, pH 7.4) three times and resuspended to 0.5×10^3~2.5×10^3 CFU/mL, then 100 μL above fungal suspension was added to a 96-well plate with a series concentration of GmAMP (100, 50, 25, 12, 6, 3 μM) or fluconazole (3,343 μM to 3 μM) (Yuan Ye, Shanghai, China) and 10 mM PBS and medium were used as the negative and blank controls, respectively. After co-incubation at 35 °C for 24 h, The drug concentration corresponding to the well without visible fungal growth was regarded as MIC, corresponding to 90% inhibition of fungal growth. The experiment was performed in triplicate and repeated three times.

Growth and fungicidal kinetics

To analyze the antifungal or fungicidal process of GmAMP against fluconazole-resistant *C. tropicalis*, the growth kinetics and time-kill kinetics of GmAMP on fluconazole-resistant *C. tropicalis* were further investigated at different times after GmAMP treatment as to previously described (*Ramesh et al., 2023*). The concentration of the prepared fungal cells

was 1.0×10^6 CFU/mL according to the previously mentioned method and incubated with 25, 50, and 100 μM of GmAMP at 35 °C for 48 h. A microplate reader (Thermo Fisher Scientific, Waltham, MA, USA) was used to record the OD_{630nm} every 2 h during co-cultivation. In the meantime, the cultivated yeasts were harvested at certain intervals (0, 2, 4, 6, 8, 10, and 12 h), and the agar solid plate experiment was conducted following gradient dilution. The negative and blank controls in the experiment were 10 mM PBS and medium. Fungal colonies were counted after incubation at 35 °C for 24 h. The results were presented as the average of triplicate measurements from three independent assays.

Effect of GmAMP on hypha formation

To analyze the effect of GmAMP on the transition of yeast-to-hyphal phase in fluconazole-resistant *C. tropicalis* as described previously (*Jiang et al., 2016*). The concentration of the prepared fungal cells was 1.0×10^6 CFU/mL in RPMI 1640 medium (Gibco, Waltham, MA, USA) which contained 15% fetal bovine serum (Gibco, Waltham, MA, USA) according to the previously mentioned method. A total of 500 μL of fungal suspension was incubated with GmAMP at concentrations (25, 50, and 100 μM) in 24 well plates and 10 mM PBS as the negative control. Cells were co-incubated with peptides for 3, 6, 9, 12, and 24 h at 37 °C, then the hypha formation was observed and photographed under an inverted microscope.

Antibiofilm assay

Fungal cells grown to the logarithmic phase were adjusted to 1.0×10^6 CFU/mL with RPMI-1640 liquid medium and added to 96-well polypropylene plates, which were then incubated at 37 °C for 90 min (biofilm formation assay) or 48 h (biofilm eradication assay) according to previous method (*Zou et al., 2024*). And 100 μL newly prepared 2, 3-bis(2-methoxy-4-nitro-5-sulfophenyl) 2H-tetrazolium5-carboxamide sodium salt (XTT) solution (Yuan Ye, Shanghai, China) was added to each well for 2 h at 37 °C after different concentrations of GmAMP were added and continued to co-incubate for 24 h. A microplate reader set to OD_{490nm} was used to measure absorbance.

Sterile polylysine cell crawls were then placed on the bottom of a 24-well plate and 500 μL of the fungal suspension at the above concentration was added. The biofilm formation and mature biofilm were prepared according to the above method, and 500 μL of SYTO 9 (Invitrogen, Waltham, MA, USA) and propidium iodide (PI; Sigma) solution with the final concentration of 10 μM were added and incubated for 20 min while 10 mM PBS was used as the negative control. Seal the cover glass with nail polish, laser confocal microscopy (Olympus SpinSR10; Olympus, Tokyo, Japan) was used to observe and obtain images.

Scanning electron microscope

The concentration of the prepared fungal cells was 1.0×10^6 CFU/mL based on the previous description with minor modifications (*Alfaro-Vargas et al., 2022*), incubated in GmAMP with culture medium at 35 °C for 2 h, and 10 mM PBS was used as a negative control, then the suspension was centrifuged at 5,000 rpm for 10 min, fixed with 2.5%

glutaraldehyde overnight at 4 °C, and dehydrated with 50%, 75%, 95% and 100% series of ethanol solutions for 10 min. It was then dried in a vacuum evaporator and coated with a thin layer of gold-palladium. The samples were observed by scanning electron microscopy and the image acquisition was performed using a Hitachi Regulus SU8100 (Tokyo, Japan).

Flow cytometry analysis

The concentration of the prepared fungal cells was 1.0×10^6 CFU/mL according to the previous description with minor modifications (*Torres et al., 2023*), the GmAMP with different concentrations was incubated at 35 °C for 1 h, and 10 mM PBS was used as the negative control. After that, the fungal suspension was incubated with SYTO 9 and PI staining with a final concentration of 10 μM at 35 °C for 15 min, and the stained cells were analyzed by flow cytometry.

Membrane potential

The concentration of the prepared fungal cells was 1.0×10^6 CFU/mL as described in the previous study (*Decker et al., 2024*), then added to 96-well plates while the membrane potential $DiSC_3(5)$ probe was added into the fungal suspension. The fungal suspension was then treated with different concentrations of GmAMP, and 10 mM PBS was used as the negative control for measured fluorescence intensity. The change of fluorescence intensity in 1 h was continuously and dynamically monitored with by RF-5301PC sectrofluoro-photometer (Bio-Tek Synergy HTX, Winooski, Vermont, USA).

Reactive oxygen species level

The levels of ROS were determined by using 2′, 7′-dichlorodihydrofluorescein diacetate (DCFH-DA; Yuan Ye, Shanghai, China) according to previously described methods (*Shaban, Patel & Ahmad, 2024*). The 1.0×10^6 CFU/mL of fungal suspension was added to 96-well plates while the Reactive Oxygen DCFH-DA probe (10 μM) was added into the fungal suspension. The fungal suspension was then treated with different concentrations of GmAMP. 10 mM PBS and 10 μM NAC (N-Acetylcysteine) were used as the negative and positive control. The change of fluorescence intensity in 1 h was continuously and dynamically monitored by RF-5301PC sectrofluoro-photometer (Bio-Tek Synergy HTX, Winooski, VT, USA).

Cytotoxicity Assays

Mouse RAW 264.7 cells were used to evaluate the cytotoxicity of GmAMP on mammalian cells as previously described (*de Oliveira et al., 2023*). Cells were cultured in Dulbecco's Modified Eagle Medium (DMEM, Gibco, Grand Island, NY, USA) containing 10% fetal bovine serum (FBS; Gibco, Waltham, MA, USA), 1% penicillin-streptomycin (Gibco, Waltham, MA, USA), and maintained at 37 °C in a humidified 5% CO_2 incubator. Firstly, 100 μL of RAW 264.7 cells suspension (2×10^4 cells/mL) was added to 96-well plates for cultivating overnight. A total of 100 μL with different concentrations of GmAMP solution was added and then incubated at 37 °C for 24 h. 10 mM PBS and complete medium were

used as the negative and blank controls, respectively. When the incubation period was over, 10 μL of CCK8 solution was added to each assay well following the manufacturer's protocols (MedChemExpress, Monmouth Junction, NJ, USA) and incubated for 1 h. Absorbance values were detected at $OD_{450nm,}$ and the percentage of cell survival was counted.

$$\text{Cell viability}(\%) = \left(\frac{\text{Abs}_{450nm}\text{of GmAMP solution} - \text{Abs}_{450nm}\text{of blank control}}{\text{Abs}_{450nm}\text{of PBS control} - \text{Abs}_{450nm}\text{of blank control}}\right) \times 100\%.$$

Hemolysis of human red blood cells

The human red blood cells (hRBCs) were used to evaluate the hemolytic activity of GmAMP based on previous descriptions with minor modifications (*Larrán et al., 2022*). The GmAMP with different concentrations and 2% hRBCs were added to the 96-well plate and incubated for 1 h in 37 °C. 1% Triton X-100 (Solarbio, Beijing, China) was the positive control, and 10 mM PBS was used as the negative control. When the incubation period was over, as the samples were gathered and centrifuged for 10 min at 1,000 rpm, the supernatant was moved to a fresh 96-well plate, and the OD_{540nm} absorbance value was used to determine the extent of hemolysis. The hemolysis test of the new peptide has been approved by Ethics Committee of GuiZhou Medical University, approval number: 2022 Ethical Approval (302).

$$\text{Hemolysis}(\%) = \left(\frac{\text{Abs}_{540nm}\text{ of GmAMP solution} - \text{Abs}_{540nm}\text{ of PBS control}}{\text{Abs}_{540nm}\text{ of (TritonX} - 100) - \text{Abs}_{540nm}\text{ of PBS control}}\right) \times 100\%.$$

Galleria mellonella infection model

The larvae used in the experiment were purchased from Huiyude Biotechnology Co., Ltd., (Tianjin, China), each weighing 250~300 mg and about 2~3 cm in length. As previously described with slight modifications (*Fernandes, Weeks & Carter, 2020*). All larvae were placed in a dark incubator at 35 °C overnight before the experiment. Ten larvae were randomly divided into each group to inject 10 μL of GmAMP solution with a concentration of 8~32 mg/kg into the last left proleg of larvae to evaluate the toxicity of GmAMP. The negative control was given an equal volume of sterile PBS. In order to assess the effectiveness of GmAMP, 12 larvae were randomly assigned to each group, and 10 μL of a fungal suspension containing roughly 5.0×10^8 CFU/mL was injected into the final left proleg of the larvae. After 1 h in the incubator, the same volume of GmAMP was injected into the last right proleg using the same method. Live and dead counts were taken every 24 h during the five days of incubation at 35 °C. Larvae were deemed dead when they went dark or mushy and had no discernible tactile reaction. Three larvae per group were chosen at random and placed into 1.5 mL of sterile PBS solution for high-speed homogenization and grinding after 24 h following GmAMP injection. The 10 μL gradient dilution was dropped onto a sterile solid YPD plate and incubated for 24 h. The number of fungal single colony was recorded, and the *C. tropical* burden of each larva was counted.

Data processing

Statistical mapping and data analysis were performed using GraphPad Prism 8.0 software (GraphPad Software). Data were expressed as mean ± SD and analyzed by one-way ANOVA. Long-rank test was used for the analysis of Mantel-Cox survival curves for the *G. mellonella* survival experiment. $P < 0.05$ was considered statistically significant.

RESULTS

GmAMP chemical characteristics

The antibacterial activity of antimicrobial peptides is significantly influenced by their secondary structure. The antimicrobial peptide's interaction with the cell membrane is facilitated by the alpha-helical structure, which increases the antibacterial activity. (*Personne et al., 2023*). The antimicrobial peptide GmAMP, composed of 21 amino acids, is predicted to have an α-helical structure (Figs. 1A and 1B). The molecular weight (MW) of GmAMP was confirmed to be 2,539.35 Da by mass spectrometry. Furthermore, GmAMP has a net charge of +17 and a hydrophobicity value of −0.757 (Fig. 1C), these characteristics imply that GmAMP is a cationic hydrophilic peptide.

Antifungal activity

The results of the antifungal activity assay showed that GmAMP had strong antimicrobial effects against clinical fluconazole-resistant *C. tropicalis*, with MICs ranging from 25 to 50 μM (Table 1). In comparison to this, the MIC values of fluconazole against *C. tropicalis* ATCC 20962 was 13.06 μM (4 μg/mL), which was consistent with the Clinical and Laboratory Standards Institute standard (CLSI). The MIC values of fluconazole against clinical isolates exceeded 3,343 μM. Consequently, to gain a more comprehensive understanding of the impact of GmAMP on fluconazole-resistant *Candida tropicalis* clinical isolate, the 4252 isolate (MIC = 25 μM) was selected for further investigation.

Growth kinetics and fungicidal kinetics

To elucidate the effect of GmAMP on the growth process of fluconazole-resistant *C. tropicalis*, the growth curve of fluconazole-resistant *C. tropicalis* under GmAMP treatment was further plotted, as shown in Fig. 2A, the fungal cells in the control group entered the logarithmic phase within 6 h and reached the stationary phase within 18 h. In comparison, GmAMP treatments at concentrations of 25 and 50 μM were found to slow down the proliferation rate of fluconazole-resistant *C. tropicalis* and prolong the time to reach the logarithmic phase. When treated with GmAMP at a concentration of 100 μM, GmAMP showed an inhibitory effect on fluconazole-resistant *C. tropicalis* and prevented the natural growth and reproduction of fluconazole-resistant *C. tropicalis*. The time-fungicidal kinetic curve was further plotted to clarify the fungicidal effect of GmAMP (Fig. 2B). Compared with the control group, GmAMP exhibited a powerful inhibitory effect on fluconazole-resistant *C. tropicalis* when the concentrations of GmAMP were 25 and 50 μM. Notably, dealing with the concentration at 100 μM of GmAMP, the fluconazole-resistant *C. tropicalis* was killed within 2 h. These results indicate that GmAMP manifests effective antimicrobial activity and fungicidal effect against

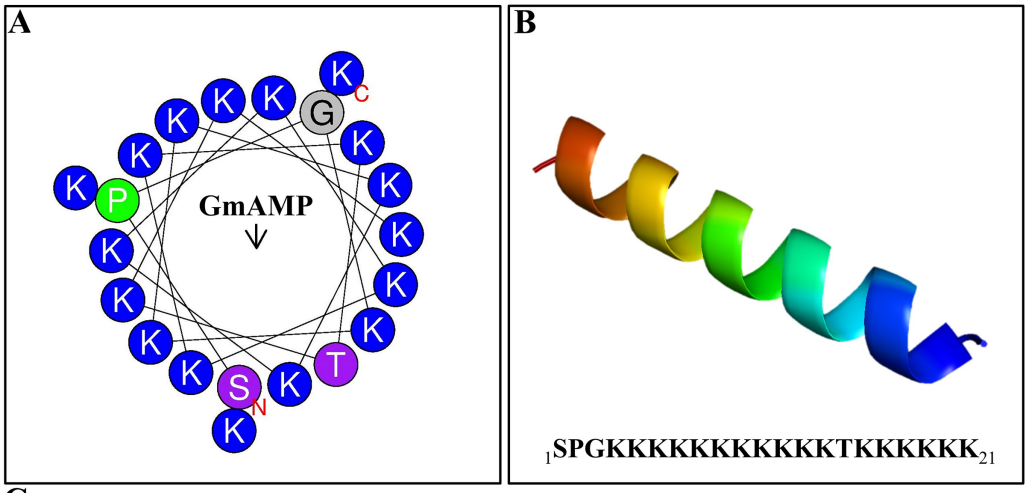

C

Peptide	Hydrophobicity <H>	Hydrophobic moment <μH>	Net charge	Theoretical MW	Measured MW
GmAMP	-0.757	0.038	+17	2539.33	2539.35

Figure 1 Physicochemical properties of GmAMP. (A) Helical wheel analysis of GmAMP. Positively charged amino acids are indicated in blue, the red 'N' represents the starting position and the arrow represents the hydrophobic moment. (B) Predicted three-dimensonal spatial structures of GmAMP. (C) The physical and chemical properties of GmAMP. Full-size DOI: 10.7717/peerj.19372/fig-1

Table 1 Antifungal activity of GmAMP. Determination of antifungal activity of GmAMP against five strains of *Candida tropicalis*.

Strains	MIC (μM)	
	GmAMP	Fluconazole
Fluconazole-resistant *C. tropicalis* 4252	25	>3,343
Fluconazole-resistant *C. tropicalis* 4171	50	>3,343
Fluconazole-resistant *C. tropicalis* 6984	50	>3,343
Fluconazole-resistant *C. tropicalis* 8402	50	>3,343
C. tropicalis ATCC 20962	12	13

fluconazole-resistant *C. tropicalis*. Low-concentration GmAMP exerts an inhibitory effect on the growth of drug-resistant *Candida tropicalis*, whereas high-concentration high GmAMP directly kills Candida cells.

The transformation of yeast to the mycelial phase

The transformation of *Candida* mycelial morphology is closely related to its pathogenicity. Morphological changes during the transformation of the fluconazole-resistant *C. tropicalis* yeast phase to the mycelial phase were observed by using an inverted microscope which is shown in Fig. 2C. The length of the mycelium of the fungus in the control group increased with incubation time, after 9 h of incubation, the yeast cells were observed to grow and

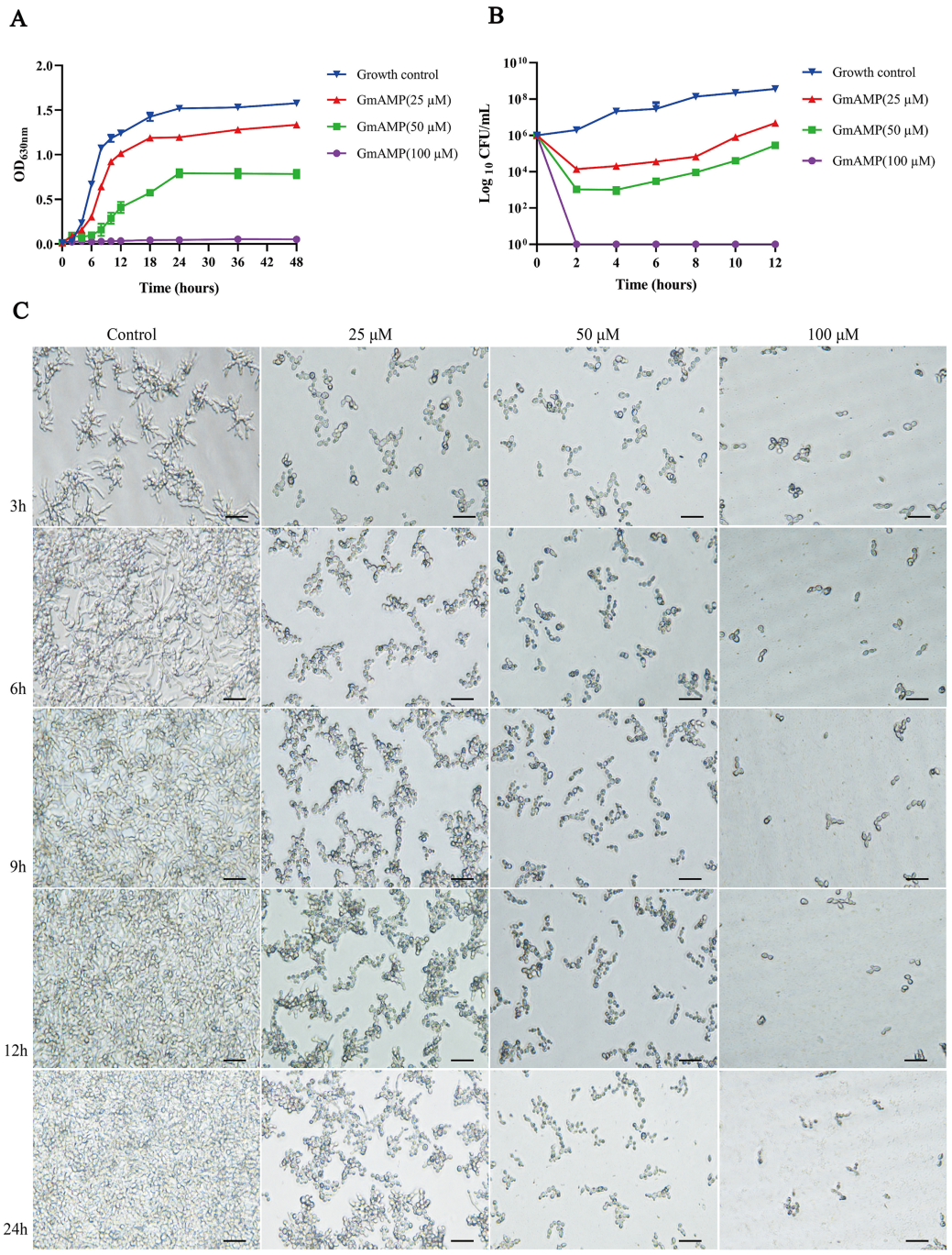

Figure 2 Effect of GmAMP on the growth of fluconazole-resistant *C. tropicalis*. (A) Growth kinetics of fluconazole-resistant *C. tropicalis*. (B) Time-killing kinetics of fluconazole-resistant *C. tropicalis*. (C) The transformation from yeast phase to mycelial phase of fluconazole-resistant *C. tropicalis*. Scale bar, 25 μm. Full-size DOI: 10.7717/peerj.19372/fig-2

form bundles of hyphae while forming branches of various sizes and lengths and intertwining with each other to form a net structure, and a more tightly netted biofilm is formed over time. Interestingly, the development of fluconazole-resistant *Candida*

tropicalis into its hyphal form was inhibited to varying degrees following treatment with GmAMP. Specifically, the morphological transformation from yeast to hyphae was partially inhibited at concentrations of 25 and 50 μM of GmAMP, whereas it was completely suppressed at a concentration of 100 μM. These results suggest that GmAMP inhibited the morphological transformation process of fluconazole-resistant *C. tropicalis* from the yeast phase to the mycelial phase.

Inhibition of biofilm formation and eradication of mature biofilm

In order to investigate whether GmAMP has an anti-*Candida tropicalis* biofilm effect, we visualized the results by using confocal laser scanning microscopy. In the control group of the biofilm formation assay, a compact and intact biofilm was observed to emit predominantly green fluorescence colored by SYTO9, a dye that penetrates cells. Nevertheless, after GmAMP treatment, intact biofilm could no longer be formed and only dispersed incomplete membranes of different sizes were observed, while only single yeast cells could be seen in the high-concentration group (Fig. 3A). In the control group of the biofilm eradication assay, it was observed that the tightly structured and complete biofilm mainly emitted green fluorescence colored by SYTO9. After GmAMP treatment, we found that the tightly structured biofilm became loose and the network structure was reduced and thinned, while a reduction in the number of yeasts and an increase in the number of fungal damages was observed, with a predominantly red fluorescence colored by PI, a dye that penetrates injured cells (Fig. 3B). In addition, the biofilm activity of *C. tropicalis* was determined by XTT quantitative method. Compared with the control group, GmAMP at concentrations of 50, 100, and 200 μM inhibited biofilm formation by 49.75%, 71.28%, and 88.32%, respectively (Fig. 3C), and eradicated mature biofilm by 17.53%, 42.07%, and 58.28%, respectively (Fig. 3D). These results indicated that GmAMP inhibited biofilm formation and eradicated a certain amount of mature biofilm in fluconazole-resistant *C. tropicalis*.

Antifungal mechanism

To investigate the impact of GmAMP on the cell morphology of fluconazole-resistant *C. tropicalis*, the morphological changes induced by GmAMP treatment of fungal cells for 2 h were directly observed by scanning electron microscopy. Untreated fungal cells were morphologically intact, with cell surfaces remaining round and smooth (Fig. 4A). When cells were exposed to 100 μM of GmAMP for 2 h, the cells were destroyed and the surface appeared rough and irregular (Fig. 4B). Thus, these outcomes suggested that the cellular structural integrity of fluconazole-resistant *C. tropicalis* has been impaired. To further investigate the interaction of GmAMP on the cell membrane of fluconazole-resistant *C. tropicalis*, PI and SYTO9 fluorescence staining were used to determine the effect of GmAMP on the integrity of the cell membrane. PI and STOY9 are DNA-binding dyes emitting red and green fluorescence, respectively, and the former only penetrated the membrane-damaged cells, while the latter stained both live and dead cells (*Jin et al., 2005*). As a result, when cells were exposed to 25, 50, and 100 μM of GmAMP, 45.02%, 76.88%, and 85.02% of the cells stained positively for PI, respectively. Moreover, PI staining

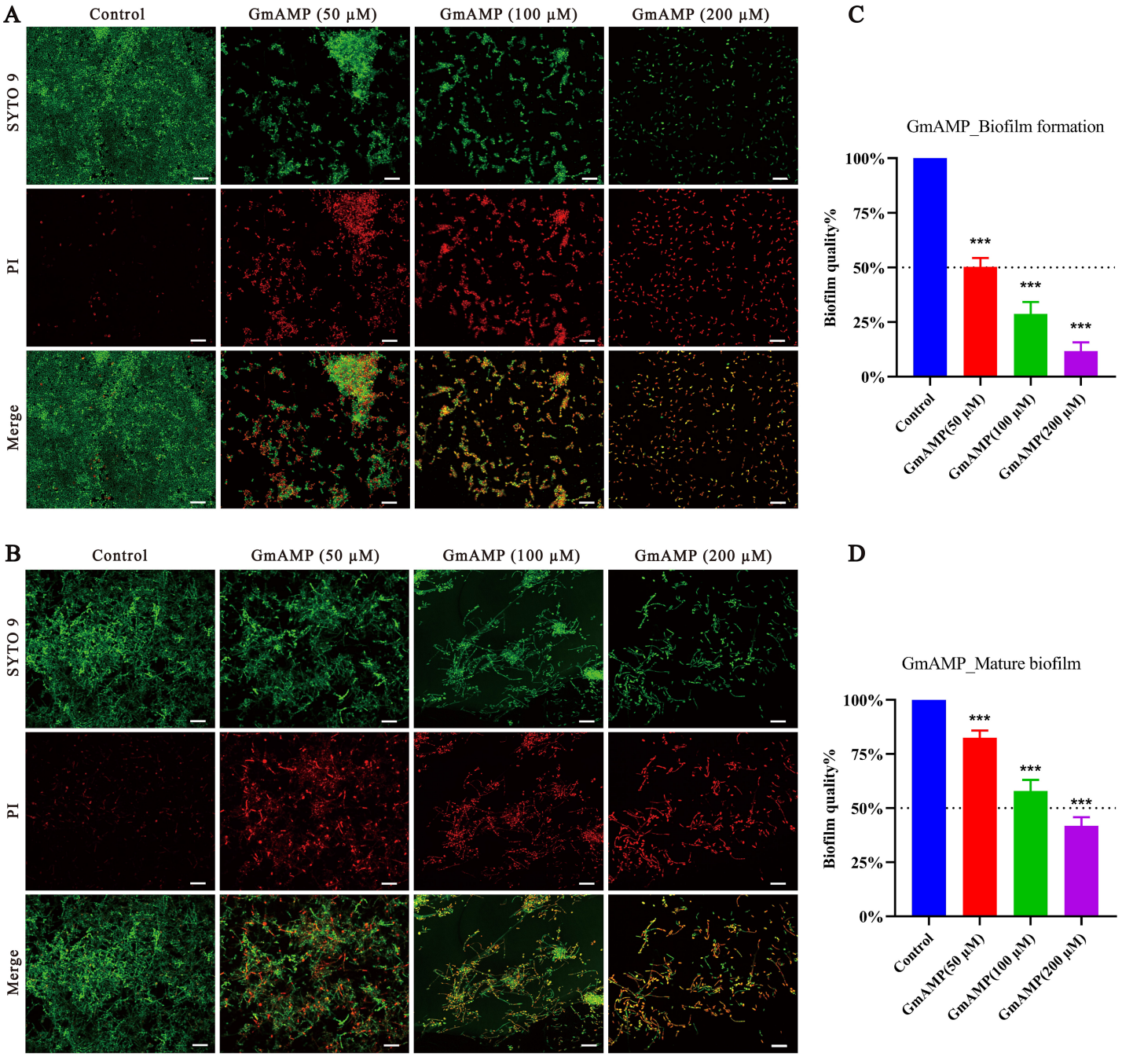

Figure 3 Effect of GmAMP on the biofilm of fluconazole-resistant *C. tropicalis*. Inhibition (A) and eradication (B) effects of fluconazole-resistant *C. tropicalis* biofilms treated with GmAMP at different concentrations observed by confocal laser scanning microscopy. Images obtained by live/dead staining (SYTO 9, green; PI, red). Scale bar, 20 μm. The activity level of biofilm under different concentrations of GmAMP was determined by the XTT reduction method (C and D), and the colorimetric absorbance was measured at OD_{490nm}. The error bar represents the standard deviation of the three independent experiments. $^{***}P < 0.001$ compared with the control group. Full-size DOI: 10.7717/peerj.19372/fig-3

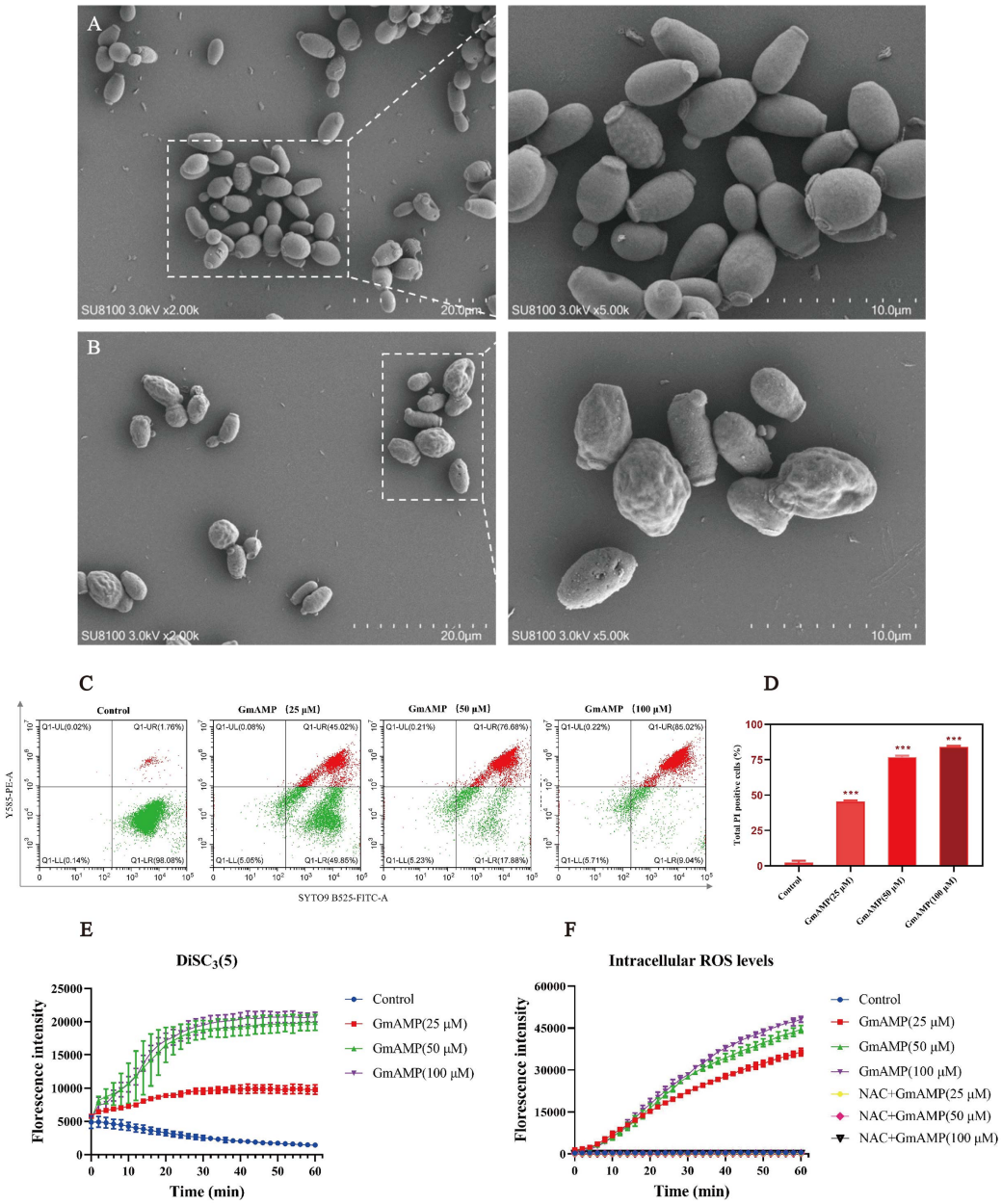

Figure 4 Effects of GmAMP cell morphology and cell membranes of fluconazole-resistant *C. tropicalis*. The control group (A) and GmAMP group treated with 100 μM (B) of fluconazole-resistant *C. tropicalis* morphological images by scanning electron microscopy. (C) Cell membrane permeability of GmAMP on the fluconazole-resistant *C. tropicalis* was determined by flow cytometry, and with SYTO 9 and PI as pore formation mechanism marker. (D) The bar chart showed the percentage of PI positive cells. (E) $DiSC_3(5)$ was used to detect the cell membrane depolarization of fluconazole-resistant *C. tropicalis*. (F) The ROS-induced accumulation of DCFH-DA is a pore formation mechanism marker. The error bar represents the standard deviation of the three independent experiments. *** $P < 0.001$ compared with the control group. Full-size DOI: 10.7717/peerj.19372/fig-4

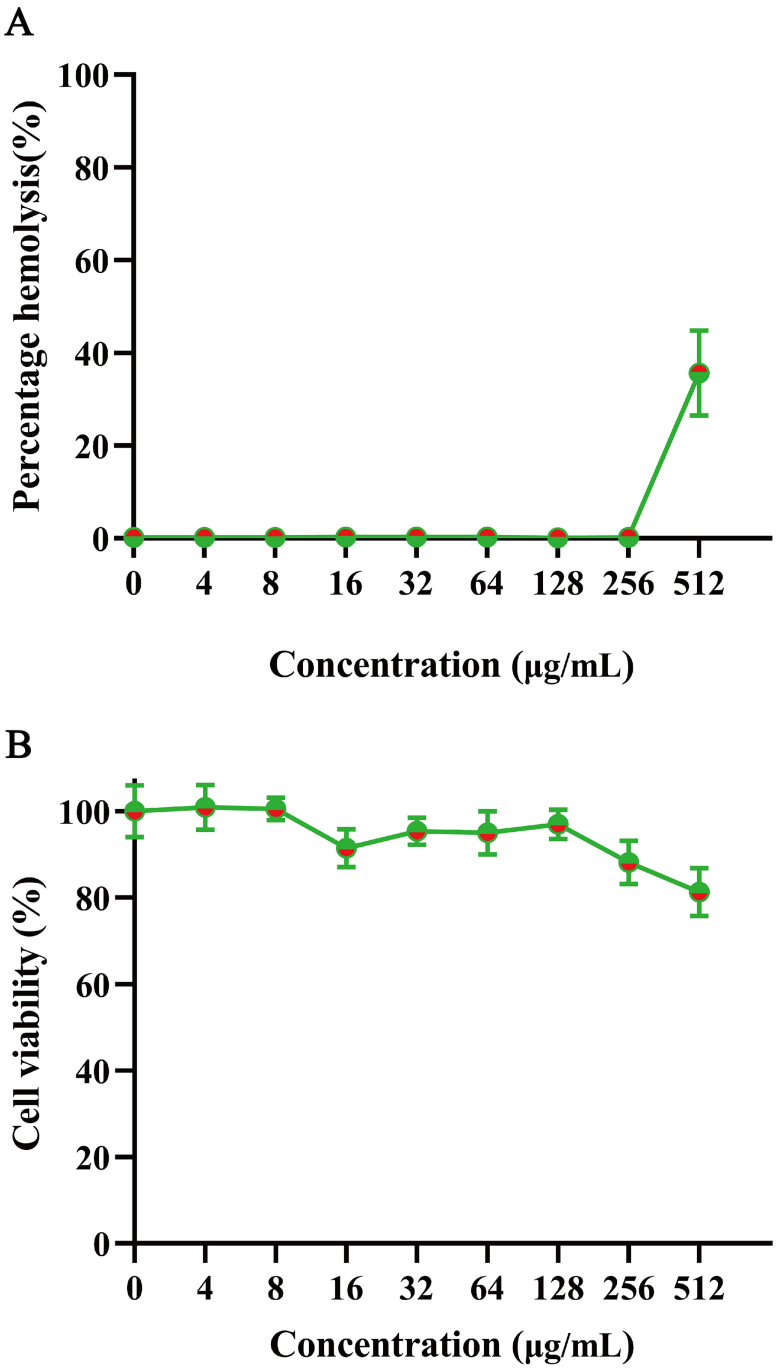

Figure 5 The hemolytsis and cytotoxicity effects of GmAMP. (A) The cytotoxicity of GmAMP against RAW 264.7 cells. (B) The hemolysis rate of 2% human red blood cells.

Full-size DOI: 10.7717/peerj.19372/fig-5

positivity showed a dose-dependent correlation with GmAMP (Fig. 4D), which indicated that GmAMP disrupted the cell membrane integrity of fluconazole-resistant *C. tropicalis*. The membrane depolarization was detected using the membrane potential probe $DiSC_3(5)$. As shown in Fig. 4E, compared with the control group, we found that GmAMP

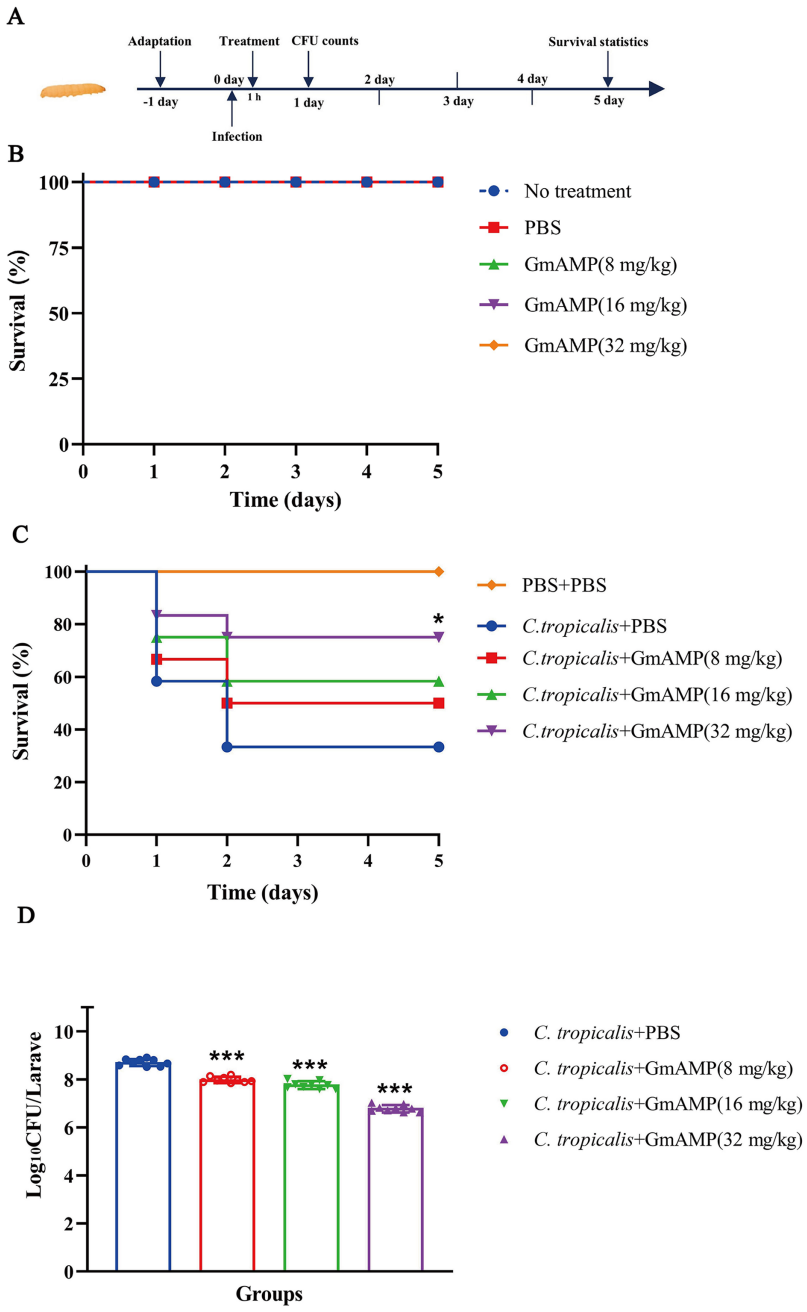

Figure 6 ***In vivo*** **toxicity and therapeutic activity of GmAMP in the *G. mellonella* model.** (A) Schematic diagram of the GmAMP treatment. (B) The toxicity of GmAMP in *G. mellonella* larvae model. (C) Survival of larvae after treatment with GmAMP. (D) Fungal burden of larvae after treatment with GmAMP. $^{*}P < 0.05$; $^{***}P < 0.001$ compared with the group of fluconazole-resistant *C. tropicalis* + PBS.
Full-size DOI: 10.7717/peerj.19372/fig-6

treatment caused depolarization of the cell membrane potential of fluconazole-resistant *C. tropicalis* and the level of membrane potential rose significantly with increasing concentration of GmAMP. Reactive oxygen species (ROS) generally maintain low levels

within normal cells, but the accumulation of higher levels of ROS can damage cellular structures (*Huang et al., 2020*). Here, different concentrations of GmAMP induced ROS accumulation in fluconazole-resistant *C. tropicalis*, and ROS levels showed a time-dose dependence (Fig. 4F). These results suggest that the presence of GmAMP induced ROS production, which contributed to the crucial factor in the antimicrobial effect of GmAMP.

Hemolytic and cytotoxicity

To evaluate mammalian cytotoxicity, we assessed the safety of GmAMP on human red blood cells and RAW 264.7 cells. The hemolysis experiment was performed using 2% human red blood cells. At a concentration of 200 μM, GmAMP exhibited slight hemolysis with a hemolysis rate of 35.64% (Fig. 5A). Moreover, GmAMP showed no obvious cytotoxicity to RAW 264.7 cells, and the cell viability of mouse macrophage RAW 264.7 remained above 80% at 200 μM concentration of GmAMP (Fig. 5B).

Therapeutic effect on fluconazole-resistant *C. tropical* infection *in vivo*

The *G. mellonella* larvae infection model was used to investigate the treatment efficacy of GmAMP *in vivo*. In the peptide toxicity test (Fig. 6B), all larvae survived, suggesting that GmAMP did not exhibit significant toxicity within the 32 mg/kg dosage range. Survival of larvae infected with fluconazole-resistant *C. tropicalis* was increased by injecting various concentrations of GmAMP, with 75% survival in the 32 mg/kg group ($P < 0.05$), whereas the control group had 40% survival rate at 5 days post infection (Fig. 6C). These results were also reflected by the fungal burden of *G. mellonella* larvae. The number of colonies per larva was significantly reduced in all treatment groups after 24 h of treatment with GmAMP, whereas 32 mg/kg GmAMP reduced the fungal burden from 5.27×10^8 to 6.37×10^6 CFU per larva (Fig. 6D). Consequently, GmAMP has the potential for clinical application as it effectively treats fluconazole-resistant *C. tropicalis* infection and reduces the fungal burden *in vivo*.

DISCUSSION

Antifungal drug resistance is currently rapidly developing due to the abuse of antibiotics, which is increasing the morbidity and fatality rate from invasive fungal infections (*Fan et al., 2024*). The isolation rate of *Candida* species, such as *Candida albicans*, *Candida glabrata*, *Candida tropicalis*, *Candida krusei*, and *Candida parapsilosis* is steadily increasing in hospitals (*Falagas, Roussos & Vardakas, 2010*; *Lee et al., 2022*). According to recent reports, China's proportion of isolates of *C. tropicalis* that are resistant to fluconazole is still increasing (*Wang et al., 2021*). The development of new antifungal drugs to address this problem is imminent. Widely distributed in animals, plants, and other organisms, AMPs are a fast and effective barrier against pathogens in humans. AMPs exert their antimicrobial activity through a unique membrane-targeting mechanism that avoids the development of drug resistance and is regarded as a novel alternative to synthetic antibiotics (*Mulukutla et al., 2024*).

In this study, we determined *in vitro* the antimicrobial activity of GmAMP against four clinical isolates of fluconazole-resistant *C. tropicalis* and the standard strain of *C. tropicalis*

ATCC 20962, and GmAMP showed good antimicrobial effect against clinical isolate of fluconazole-resistant *C. tropicalis* 4252, with a MIC value of 25 μM. GmAMP not only delayed the proliferation rate and inhibited the growth and reproduction of fungi, but also effectively killed *C. tropicalis* within 2 h. These results suggest that GmAMP is an effective antimicrobial agent and further studies on the antifungal efficacy of GmAMP are necessary.

The process of transformation from the yeast phase to the mycelial phase, termed "biphasic", is considered the most important pathogenic characteristic of *Candida*, and is also recognized as a key stage in biofilm formation and maturation (*Zhu et al., 2024*). Furthermore, the hyphae formed during the morphological transformation can penetrate cells and invade the bloodstream, expressing a wide range of virulence factors, and they are regarded as a more virulent phenotype than yeast (*Khamzeh et al., 2023*). Herein, GmAMP inhibited the transition of yeast phase cells to mycelial phase morphology, preventing the process of mycelial development, which demonstrates that GmAMP plays a key role in inhibiting the formation and maturation of fluconazole-resistant *C. tropicalis* biofilm by preventing mycelial development. The yeast cells of *C. tropicalis* are characterized by a high capacity to form biofilms compared to other *Candida* species (*Zuza-Alves, Silva-Rocha & Chaves, 2017*), which may be related to an increased amount of biomass in the membranes and extracellular matrix, leading to a denser structure (*Chandra & Mukherjee, 2015*; *Desai & Mitchell, 2015*). Here, the 50 μM (2 × MIC) of GmAMP inhibits biofilm formation and has an eradicative effect on mature biofilms. Moreover, GmAMP inhibited and eliminated biofilms of fluconazole-resistant *C. tropicalis* in a concentration-dependent manner. Therefore, GmAMP showed good bioactivity in inhibiting morphological transformation and anti-biofilm processes.

It has been reported that most antimicrobial peptides exert their antimicrobial effects mainly by targeting cell membranes (*Aguiar et al., 2020*; *Buda De Cesare et al., 2020*; *Hu et al., 2022*). In the present study, the results of the scanning electron microscopy assay demonstrated that GmAMP disrupts the morphology and structure of the fluconazole-resistant *C. tropicalis*. A similar phenomenon was also found by *Ma et al. (2020)*, *Zhang et al. (2023)*. Moreover, we speculated the exact reason for the morphological damage and subsequent cell death is correlated with increased membrane permeability resulting from electrostatic interactions between the positively charged peptide GmAMP and the negatively charged components of the fungal cytoplasmic membrane (*Boparai & Sharma, 2020*; *Jayasinghe, Whang & De Zoysa, 2023*; *Kodedová et al., 2019*). The experimental result verified membrane permeability by a significant increase in the number of PI-stained positive cells of the fungi treated with GmAMP. Changes in cell membrane permeability usually trigger variation in cell membrane potential, which is closely related to cellular function (*D'Auria et al., 2022*). When membrane-modifying compounds (*e.g.*, peptides) depolarize the membrane then the potential is lost. $DiSC_3(5)$ is released into the solution, causing fluorescence enhancement, which indicates that the cytoplasmic membrane is altered because of the cell membrane depolarization by the action of GmAMP in a concentration-dependent manner, which suggests that the dissipation of membrane potential might be involved in the formation of

channels or pores, then allowed the passage of ions or macromolecules, to lead cytoplasmic membrane dysfunction (*Bezerra et al., 2022*; *Venkatesh et al., 2017*). It has been found that aerobic metabolism-generated ROS are usually present in cells that are in equilibrium with antioxidant enzymes, and excess ROS have certain deleterious effects on the basic structure of fungi, such as damage to nucleic acids, DNA, amino acid residues, and cell membranes (*Perrone, Tan & Dawes, 2008*). We found that GmAMP induced the accumulation of reactive oxygen species in a dose-dependent manner (*Taveira et al., 2022*). In brief, we hypothesized that the cationic peptide GmAMP can interact with certain negatively charged substance molecules on the cell membrane through electrostatic interactions, it leads to a series of consequences such as increased membrane permeability, altered depolarization of the membrane potential, structural loss of membrane integrity, accumulation of ROS, and further leakage of intracellular contents, which finally leads to cytoplasmic membrane dysfunction and cell death.

The excellent antimicrobial activity of antimicrobial peptides is usually associated with strong hemolytic activity and cytotoxicity, and assessment of the *in vitro* safety of AMP is paramount for further consideration as a potential clinical candidate (*Zhang et al., 2024*). In this study, our results showed that GmAMP showed little cytotoxicity and low hemolytic effect. Although some cytotoxicity and hemolytic activity were observed at higher concentrations, considering the MIC value of GmAMP was 25 μM (Table 1), which was much lower than its cytotoxicity concentration, GmAMP safety is also guaranteed under the premise of ensuring its activity. However, the potential toxicity of GmAMP to other mammalian cells remains to be studied.

The safe and effective dose range of GmAMP is confirmed by cytotoxicity and hemolytic tests, laying the foundation for its application in animal studies. In this study, the therapeutic efficacy of GmAMP was tested *in vivo* using the *G. mellonella* larvae infection model, which showed a significant improvement in survival. The fungal burden of *G. mellonella* larvae was considerably decreased *in vivo* with GmAMP therapy. These findings suggest that GmAMP may exhibit a strong safety and certain therapeutic potential.

CONCLUSIONS

This work describes the antifungal activity and mechanism of antimicrobial peptide GmAMP and therapeutic efficacy *in vivo*. GmAMP possesses potent antimicrobial activity, anti-biofilm formation, and eradication ability, and may play an antimicrobial role by disrupting the structure of fungal cytomembrane. Here, GmAMP displays low cytotoxicity and low hemolytic activity *in vitro* experiments. Furthermore, GmAMP exhibits a therapeutic effect against fluconazole-resistant *C. tropical* infection and reduces the number of fungi *in vivo*. These properties make GmAMP a potential treatment for fluconazole-resistant *C. tropical* infection, which is worthy of further optimization and development. Furthermore, GmAMP provides further opportunities for the safe and effective clinical application of antimicrobial peptides in the development of drug resistance.

ADDITIONAL INFORMATION AND DECLARATIONS

Funding

This research received funding from the National Natural Science Foundation of China (No. 81760647, 82360700), Science and Technology Planning Project of Guizhou Province (ZK[2022] general project 345), Excellent Young Talents Plan of Guizhou Medical University (No. [2021]104) and Guizhou Key Laboratory (ZDSYS[2023]004). The funders had no role in study design, data collection and analysis, decision to publish, or preparation of the manuscript.

Grant Disclosures

The following grant information was disclosed by the authors:
National Natural Science Foundation of China: 81760647 and 82360700.
Science and Technology Planning Project of Guizhou Province: ZK[2022]345.
Excellent Young Talents Plan of Guizhou Medical University: [2021]104.
Guizhou Key Laboratory: ZDSYS[2023]004.

Competing Interests

The authors declare that they have no competing interests.

Author Contributions

- Ruxia Cai conceived and designed the experiments, performed the experiments, analyzed the data, prepared figures and/or tables, authored or reviewed drafts of the article, and approved the final draft.
- Na Zhao conceived and designed the experiments, performed the experiments, prepared figures and/or tables, authored or reviewed drafts of the article, and approved the final draft.
- Chaoqin Sun performed the experiments, analyzed the data, prepared figures and/or tables, and approved the final draft.
- Mingjiao Huang performed the experiments, prepared figures and/or tables, and approved the final draft.
- Zhenlong Jiao analyzed the data, prepared figures and/or tables, and approved the final draft.
- Jian Peng performed the experiments, prepared figures and/or tables, and approved the final draft.
- Jin Zhang analyzed the data, authored or reviewed drafts of the article, and approved the final draft.
- Guo Guo conceived and designed the experiments, authored or reviewed drafts of the article, and approved the final draft.

Data Availability

The following information was supplied regarding data availability:

The raw measurements are available in the Supplemental Files.

Supplemental Information

Supplemental information for this article can be found online at http://dx.doi.org/10.7717/peerj.19372#supplemental-information.

REFERENCES

Aguiar FLL, Santos NC, de Paula CCS, Andreu D, Baptista GR, Gonçalves S. 2020. Antibiofilm activity on *Candida albicans* and mechanism of action on biomembrane models of the antimicrobial peptide Ctn[15–34]. *International Journal of Molecular Sciences* **21(21)**:8339 DOI 10.3390/ijms21218339.

Alfaro-Vargas P, Bastos-Salas A, Muñoz-Arrieta R, Pereira-Reyes R, Redondo-Solano M, Fernández J, Mora-Villalobos A, López-Gómez JP. 2022. Peptaibol production and characterization from *Trichoderma asperellum* and their action as biofungicide. *Journal of Fungi* **8(10)**:1037 DOI 10.3390/jof8101037.

Badiee P, Boekhout T, Haddadi P, Mohammadi R, Ghadimi-Moghadam A, Soltani J, Zarei Mahmoudabadi A, Ayatollahi Mousavi SA, Najafzadeh MJ, Diba K, Salimi-Khorashad AR, Amin Shahidi M, Ghasemi F, Jafarian H. 2022. Epidemiology and antifungal susceptibility of candida species isolated from 10 tertiary care hospitals in Iran. *Microbiology Spectrum* **10(6)**:e0245322 DOI 10.1128/spectrum.02453-22.

Bezerra LP, Freitas CDT, Silva AFB, Amaral JL, Neto NAS, Silva RGG, Parra ALC, Goldman GH, Oliveira JTA, Mesquita FP, Souza PFN. 2022. Synergistic antifungal activity of synthetic peptides and antifungal drugs against *Candida albicans* and *C. parapsilosis* biofilms. *Antibiotics* **11(5)**:553 DOI 10.3390/antibiotics11050553.

Boparai JK, Sharma PK. 2020. Mini review on antimicrobial peptides, sources, mechanism and recent applications. *Protein & Peptide Letters* **27(1)**:4–16 DOI 10.2174/0929866526666190822165812.

Buda De Cesare G, Cristy SA, Garsin DA, Lorenz MC. 2020. Antimicrobial peptides: a new frontier in antifungal therapy. *mBio* **11(6)**:847 DOI 10.1128/mBio.02123-20.

Chandra J, Mukherjee PK. 2015. Candida biofilms: development, architecture, and resistance. *Microbiology Spectrum* **5(3)**:MB-0020-2015 DOI 10.1128/microbiolspec.mb-0020-2015.

Clinical and Laboratory Standards Institute (CLSI). 2023. *Performance standards for antimicrobial susceptibility testing*. Wayne, PA: CLSI, M100-Ed33. *Available at https://clsi.org/standards/products/microbiology/documents/m100/*.

de Oliveira AS, de Oliveira JS, Kumar R, Silva FBA, Fernandes MR, Nobre FD, Costa ADC, Albuquerque P, Sidrim JJC, Rocha MFG, Santos FA, Srivastava V, Romeiro LAS, Brilhante RSN. 2023. Antifungal activity of sustainable histone deacetylase inhibitors against planktonic cells and biofilms of *Candida* spp. and *Cryptococcusneoformans*. *Medical Mycology* **61(8)**:877 DOI 10.1093/mmy/myad073.

Decker T, Rautenbach M, Khan S, Khan W. 2024. Antibacterial efficacy and membrane mechanism of action of the *Serratia*-derived non-ionic lipopeptide, serrawettin W2-FL10. *Microbiology Spectrum* **12(7)**:e0295223 DOI 10.1128/spectrum.02952-23.

Desai JV, Mitchell AP. 2015. Candida albicans biofilm development and its genetic control. *Microbiology Spectrum* **7(3)**:MB-0005-2014 DOI 10.1128/microbiolspec.mb-0005-2014.

D'Auria FD, Casciaro B, De Angelis M, Marcocci ME, Palamara AT, Nencioni L, Mangoni ML. 2022. Antifungal activity of the frog skin peptide temporin G and its effect on *Candida albicans* virulence factors. *International Journal of Molecular Sciences* **23(11)**:6345 DOI 10.3390/ijms23116345.

Falagas ME, Roussos N, Vardakas KZ. 2010. Relative frequency of albicans and the various non-albicans Candida spp among candidemia isolates from inpatients in various parts of the world: a systematic review. *International Journal of Infectious Diseases* **14(11)**:e954–966 DOI 10.1016/j.ijid.2010.04.006.

Fan X, Dai RC, Zhang S, Geng YY, Kang M, Guo DW, Mei YN, Pan YH, Sun ZY, Xu YC, Gong J, Xiao M. 2024. Author correction: tandem gene duplications contributed to high-level azole resistance in a rapidly expanding Candida tropicalis population. *Nature Communications* **15**:587 DOI 10.1038/s41467-024-44825-y.

Fan X, Tsui CKM, Chen X, Wang P, Liu ZJ, Yang CX. 2023. High prevalence of fluconazole resistant *Candida tropicalis* among candiduria samples in China: an ignored matter of concern. *Frontiers in Microbiology* **14**:1125241 DOI 10.3389/fmicb.2023.1125241.

Fernandes KE, Weeks K, Carter DA. 2020. Lactoferrin is broadly active against yeasts and highly synergistic with Amphotericin B. *Antimicrobial Agents and Chemotherapy* **64(5)**:292 DOI 10.1128/AAC.02284-19.

Fisher MC, Denning DW. 2023. The WHO fungal priority pathogens list as a game-changer. *Nature Reviews Microbiology* **21(4)**:211–212 DOI 10.1038/s41579-023-00861-x.

Forastiero A, Mesa-Arango AC, Alastruey-Izquierdo A, Alcazar-Fuoli L, Bernal-Martinez L, Pelaez T, Lopez JF, Grimalt JO, Gomez-Lopez A, Cuesta I, Zaragoza O, Mellado E. 2013. *Candida tropicalis* antifungal cross-resistance is related to different azole target (Erg11p) modifications. *Antimicrobial Agents and Chemotherapy* **57(10)**:4769–4781 DOI 10.1128/AAC.00477-13.

Gan BH, Gaynord J, Rowe SM, Deingruber T, Spring DR. 2021. The multifaceted nature of antimicrobial peptides: current synthetic chemistry approaches and future directions. *Chemical Society Reviews* **50(13)**:7820–7880 DOI 10.1039/D0CS00729C.

Hu N, Mo XM, Xu SN, Tang HN, Zhou YH, Li L, Zhou HD. 2022. A novel antimicrobial peptide derived from human BPIFA1 protein protects against *Candida albicans* infection. *Innate Immunity* **28(2)**:67–78 DOI 10.1177/17534259221080543.

Huang Y, Fujii K, Chen X, Iwatani S, Chibana H, Kojima S, Kajiwara S. 2020. Fungal NOX is an essential factor for induction of TG2 in human hepatocytes. *Medical Mycology* **58(5)**:679–689 DOI 10.1093/mmy/myz105.

Jayasinghe JNC, Whang I, De Zoysa M. 2023. Antifungal efficacy of antimicrobial peptide octominin II against *Candida albicans*. *International Journal of Molecular Sciences* **24(18)**:14053 DOI 10.3390/ijms241814053.

Jiang C, Li Z, Zhang L, Tian Y, Dong D, Peng Y. 2016. Significance of hyphae formation in virulence of *Candida tropicalis* and transcriptomic analysis of hyphal cells. *Microbiological Research* **192(7)**:65–72 DOI 10.1016/j.micres.2016.06.003.

Jin Y, Zhang T, Samaranayake YH, Fang HH, Yip HK, Samaranayake LP. 2005. The use of new probes and stains for improved assessment of cell viability and extracellular polymeric substances in *Candida albicans* biofilms. *Mycopathologia* **159(3)**:353–360 DOI 10.1007/s11046-004-6987-7.

Khamzeh A, Dahlstrand Rudin A, Venkatakrishnan V, Stylianou M, Sanchez Klose FP, Urban CF, Björnsdottir H, Bylund J, Christenson K. 2023. High levels of short chain fatty acids secreted by *Candida albicans* hyphae induce neutrophil chemotaxis via free fatty acid receptor 2. *Journal of Leukocyte Biology* **115(3)**:536–546 DOI 10.1093/jleuko/qiad146.

Kodedová M, Valachovič M, Csáky Z, Sychrová H. 2019. Variations in yeast plasma-membrane lipid composition affect killing activity of three families of insect antifungal peptides. *Cellular Microbiology* **21(12)**:e13093 DOI 10.1111/cmi.13093.

Larrán B, López-Alonso M, Miranda M, Pereira V, Rigueira L, Suárez ML, Herrero-Latorre C. 2022. Measuring haemolysis in cattle serum by direct UV-VIS and RGB digital image-based methods. *Scientific Reports* **12**:13523 DOI 10.1038/s41598-022-17842-4.

Lee JK, Park S, Kim YM, Guk T, Choi JK, Kim JY, Lee MY, Jang MK, Park SC. 2022. Antifungal and anti-inflammatory activities of PS1-2 peptide against fluconazole-resistant *Candida albicans*. *Antibiotics* **11(12)**:1779 DOI 10.3390/antibiotics11121779.

Lee Y, Puumala E, Robbins N, Cowen LE. 2021. Antifungal drug resistance: molecular mechanisms in *Candida albicans* and beyond. *Chemical Reviews* **121(6)**:3390–3411 DOI 10.1021/acs.chemrev.0c00199.

Li R, Zhao J, Huang L, Yi Y, Li A, Li D, Tao M, Liu Y. 2020. Antimicrobial peptide CGA-N12 decreases the *Candida tropicalis* mitochondrial membrane potential via mitochondrial permeability transition pore. *Bioscience Reports* **40(5)**:14 DOI 10.1042/BSR20201007.

Liu Y, Chen Z, Li J, Zhu Z, Pang S, Xu J, Wu J. 2022. Extensive diversity and prevalent fluconazole resistance among environmental yeasts from tropical China. *Genes* **13(3)**:444 DOI 10.3390/genes13030444.

Ma H, Zhao X, Yang L, Su P, Fu P, Peng J, Yang N, Guo G. 2020. Antimicrobial peptide AMP-17 affects *Candida albicans* by disrupting its cell wall and cell membrane integrity. *Infection and Drug Resistance* **13**:2509–2520 DOI 10.2147/idr.S250278.

McCarthy MW, Walsh TJ. 2017. Drug development challenges and strategies to address emerging and resistant fungal pathogens. *Expert Review of Anti-Infective Therapy* **15(6)**:577–584 DOI 10.1080/14787210.2017.1328279.

Mulukutla A, Shreshtha R, Kumar Deb V, Chatterjee P, Jain U, Chauhan N. 2024. Recent advances in antimicrobial peptide-based therapy. *Bioorganic Chemistry* **145(1963)**:107151 DOI 10.1016/j.bioorg.2024.107151.

Pathakumari B, Liang G, Liu W. 2020. Immune defence to invasive fungal infections: a comprehensive review. *Biomedicine & Pharmacotherapy* **130(165)**:110550 DOI 10.1016/j.biopha.2020.110550.

Perrone GG, Tan SX, Dawes IW. 2008. Reactive oxygen species and yeast apoptosis. *Biochimica et Biophysica Acta (BBA)—Molecular Cell Research* **1783(7)**:1354–1368 DOI 10.1016/j.bbamcr.2008.01.023.

Personne H, Paschoud T, Fulgencio S, Baeriswyl S, Köhler T, van Delden C, Stocker A, Javor S, Reymond JL. 2023. To fold or not to fold: diastereomeric optimization of an α-helical antimicrobial peptide. *Journal of Medicinal Chemistry* **66(11)**:7570–7583 DOI 10.1021/acs.jmedchem.3c00460.

Pfaller MA, Diekema DJ. 2007. Epidemiology of invasive candidiasis: a persistent public health problem. *Clinical Microbiology Reviews* **20(1)**:133–163 DOI 10.1128/CMR.00029-06.

Ramesh S, Madduri M, Rudramurthy SM, Roy U. 2023. Functional characterization of a bacillus-derived novel broad-spectrum antifungal lipopeptide variant against *Candida tropicalis* and *Candida auris* and unravelling its mode of action. *Microbiology Spectrum* **11(2)**:e0158322 DOI 10.1128/spectrum.01583-22.

Sasani E, Khodavaisy S, Rezaie S, Salehi M, Yadegari MH. 2021. The relationship between biofilm formation and mortality in patients with *Candida tropicalis* candidemia. *Microbial Pathogenesis* **155(5)**:104889 DOI 10.1016/j.micpath.2021.104889.

Shaban S, Patel M, Ahmad A. 2024. Antifungal activity of human antimicrobial peptides targeting apoptosis in Candida auris. *Journal of Medical Microbiology* **73(5)**:e001835 DOI 10.1099/jmm.0.001835.

Taveira GB, de Oliveira Mello É, Simão T, Cherene MB, de Oliveira Carvalho A, Muzitano MF, Lassounskaia E, Pireda S, de Castro Miguel E, Basso LGM, Da Cunha M, da Motta OV, Gomes VM. 2022. A new bioinspired peptide on defensin from *C. annuum* fruits: Antimicrobial activity, mechanisms of action and therapeutical potential. *Biochimica et Biophysica Acta (BBA)—General Subjects* **1866(11)**:130218 DOI 10.1016/j.bbagen.2022.130218.

Torres R, Barreto-Santamaría A, Arévalo-Pinzón G, Firacative C, Gómez BL, Escandón P, Patarroyo MA, Muñoz JE. 2023. In vitro antifungal activity of three synthetic peptides against *Candida auris* and other *Candida* species of medical importance. *Antibiotics* **12(8)**:1234 DOI 10.3390/antibiotics12081234.

Tseng KY, Liao YC, Chen FC, Chen FJ, Lo HJ. 2022. A predominant genotype of azole-resistant *Candida tropicalis* clinical strains. *The Lancet Microbe* **3(9)**:e646 DOI 10.1016/S2666-5247(22)00179-3.

Venkatesh M, Barathi VA, Goh ETL, Anggara R, Fazil M, Ng AJY, Harini S, Aung TT, Fox SJ, Liu S, Yang L, Barkham TMS, Loh XJ, Verma NK, Beuerman RW, Lakshminarayanan R. 2017. Antimicrobial activity and cell selectivity of synthetic and biosynthetic cationic polymers. *Antimicrobial Agents and Chemotherapy* **61(10)**:e00469 DOI 10.1128/aac.00469-17.

Wang Y, Fan X, Wang H, Kudinha T, Mei YN, Ni F, Pan YH, Gao LM, Xu H, Kong HS, Yang Q, Wang WP, Xi HY, Luo YP, Ye LY, Xiao M. 2021. Continual decline in azole susceptibility rates in *Candida tropicalis* over a 9-year period in China. *Frontiers in Microbiology* **12**:702839 DOI 10.3389/fmicb.2021.702839.

World Health Organization (WHO) ARDA, Control of Neglected Tropical Diseases (NTD), Global Coordination and Partnership (GCP). 2022. WHO fungal priority pathogens list to guide research, development and public health action. *Available at https://www.who.int/publications/i/item/9789240060241*.

Zhang H, Chen Q, Xie J, Cong Z, Cao C, Zhang W, Zhang D, Chen S, Gu J, Deng S, Qiao Z, Zhang X, Li M, Lu Z, Liu R. 2023. Switching from membrane disrupting to membrane crossing, an effective strategy in designing antibacterial polypeptide. *Science Advances* **9(4)**:eabn0771 DOI 10.1126/sciadv.abn0771.

Zhang J, Yang L, Tian Z, Zhao W, Sun C, Zhu L, Huang M, Guo G, Liang G. 2022. Large-scale screening of antifungal peptides based on quantitative structure-activity relationship. *ACS Medicinal Chemistry Letters* **13(1)**:99–104 DOI 10.1021/acsmedchemlett.1c00556.

Zhang H, Zhang S, Wang P, Qin Y, Wang H. 2017. Forecasting of particulate matter time series using wavelet analysis and wavelet-ARMA/ARIMA model in Taiyuan. *Journal of the Air & Waste Management Association* **67(7)**:776–788 DOI 10.1080/10962247.2017.1292968.

Zhang LM, Zhou SW, Huang XS, Chen YF, Mwangi J, Fang YQ, Du T, Zhao M, Shi L, Lu QM. 2024. Blap-6, a novel antifungal Peptide from the Chinese medicinal beetle *Blaps rhynchopetera* against *Cryptococcus* neoformans. *International Journal of Molecular Sciences* **25(10)**:5336 DOI 10.3390/ijms25105336.

Zhu X, Jin F, Yang G, Zhuang T, Zhang C, Zhou H, Niu X, Wang H, Wu D. 2024. Mitochondrial protease oct1p regulates mitochondrial homeostasis and influences pathogenicity through affecting hyphal growth and biofilm formation activities in *Candida albicans*. *Journal of Fungi* **10**:391 DOI 10.3390/jof10060391.

Zou K, Yin K, Ren S, Zhang R, Zhang L, Zhao Y, Li R. 2024. Activity and mechanism of action of antimicrobial peptide ACPs against *Candida albicans*. *Life Sciences* **350(6)**:122767 DOI 10.1016/j.lfs.2024.122767.

Zuza-Alves DL, Silva-Rocha WP, Chaves GM. 2017. An update on *Candida tropicalis* based on basic and clinical approaches. *Frontiers in Microbiology* **8**:1927 DOI 10.3389/fmicb.2017.01927.